A Compact Broadband Dual-Polarized Antenna Array for Base Stations

Qianyun Zhang, *Student Member, IEEE*, and Yue Gao, *Senior Member, IEEE*

***Abstract*—A compact $\pm 45^{\circ}$ dual-polarized broadband antenna array is proposed in this letter for base stations. For the sake of structural simplicity, low profile, and ease of mass production, printed dipoles are adopted as the dual-polarized antenna element. To achieve the broadband performance, radiators are designed to be spline-edged bowties, and they are fed by tapered transmission lines. Moreover, to improve the symmetry and stability of the radiation pattern, the Pawsey stub baluns are used to balance the antenna structure. Finally, an eight-element antenna array prototype backed by a folded reflector is fabricated and measured. The compact antenna array has a broad bandwidth of 68% (1.427–2.9 GHz) with a voltage standing-wave ratio less than 1.5 and stable radiation properties to provide international mobile telecommunication services over 2G/3G/LTE systems and *L*- and *S*-bands released recently.**

***Index Terms*—Antenna array, base station antenna, broadband antenna, dual-polarized antenna.**

I. Introduction

With the extensive increase of global mobile data traffic, the demand for communication bandwidth (BW) is growing intensively. Recently, the *L*-band from 1.427 to 1.518 GHz and the *S*-band from 2.7 to 2.9 GHz have been released for international mobile telecommunication (IMT) services [1], [2]. Due to the extension of an operating frequency band, the existing base station antennas [3]–[6] cannot meet the new IMT demand, and therefore, base station antennas working continuously from 1.427 to 2.9 GHz are expected to support multiple communication systems. In addition, dual-polarized antennas are widely used for base stations to increase the polarization diversity and to improve the system performance. Furthermore, base stations nowadays tend to be increasingly compact for easy deployment, and as a result, antennas designed for them should also be compact.

The patch antenna is welcomed for the compactness, thanks to its low profile and ease of mass fabrication. However, restricted by its inherent nature of the narrow BW, patch antennas often need multiple layers and complicated feeding structures [3], [4] to achieve wideband performance, which increases the structural complexity and reduces the antenna efficiency. A dipole antenna and its variations are another popular choice for wideband base stations. In [5], two pairs of long dipoles and two pairs of short dipoles printed on an oriental crown-shaped substrate were fed differentially. Performance of this antenna is stable within the frequency band from 1.71 to 2.69 GHz (VSWR$<$1.5), yet its nonplanar structure increases the fabrication difficulties and costs. In [6], a dual-polarized base station operating over 1.71–2.69 GHz was achieved by using a crossed dipole together with a square loop and a square plate serving as the parasitic radiator and the director, respectively. Although a series of efforts, including dipole arm transformations [7], [8], designs of feeding structures [5], [9], and adding parasitic components [6], have been made to achieve broadband base station antennas with compact size, to the best of the authors' knowledge, none of the previous work realizes a fractional BW over 60% with VSWR$<$1.5.

TABLE I
BWs and Sizes of Broadband Base Station Antennas

Ref.	BW (GHz)	BW (%)	Element size (mm^3)
[4]	1.71-2.71	45	$280 \times 280 \times 32$
[5]	1.71-2.69	45	$130 \times 130 \times 71.2$
[6]	1.71-2.69	45	$70 \times 70 \times 53$
[7]	1.63-2.9	56	$134 \times 200 \times 36$
[8]	1.63-2.95	58	$145 \times 300 \times 34.7$
[9]	1.6-2.9	58	$156 \times 105 \times 42$
Proposed	1.427-2.9	68	$134 \times 110 \times 33$

In this letter, a $\pm 45^{\circ}$ dual-polarized compact antenna element and its eight-element array are designed for base stations. Operating from 1.427 to 2.9 GHz, the proposed antenna covers 2G, 3G, and LTE bands, but also recently released *L*- and *S*-bands. With a balanced structure, the proposed antenna exhibits a symmetric radiation property and achieves a stable half-power beamwidth (HPBW), good cross-polarization discrimination (XPD), and high front–back ratio (FBR) over the entire operating frequency.

II. Design of a Dual-polarized Antenna Element

A. Antenna Configuration

BWs for VSWR$<$1.5 of representative broadband base station antennas are summarized in Table I together with sizes of the antenna elements. According to Chu's theory [10], the maximum BW of an antenna is constrained by its electrical length, wherefore it is challenging to achieve the desired BW using conventional structures without losing compactness. Two crossed bowtie dipoles consisting of an isosceles triangle attached with a semicircle were used in [7] as an antenna element, and its 1×8 array achieved a BW of 56%. In this letter, we further improve the bowtie structure to obtain even broader BW within a compact size. As illustrated in Fig. 1(a) and (b), a novel bowtie is

Manuscript received March 18, 2018; revised April 17, 2018; accepted April 27, 2018. Date of publication May 3, 2018; date of current version June 4, 2018. This work was supported in part by Huawei Technologies Co., Ltd., and in part by the Engineering and Physical Sciences Research Council in the U.K. under Grant EP/R00711X/1. *(Corresponding author: Qianyun Zhang.)*

The authors are with the School of Electronic Engineering and Computer Science, Queen Mary University of London, London E1 4NS, U.K. (e-mail: qianyun.zhang@qmul.ac.uk; yue.gao@ieee.org).

Digital Object Identifier 10.1109/LAWP.2018.2832293

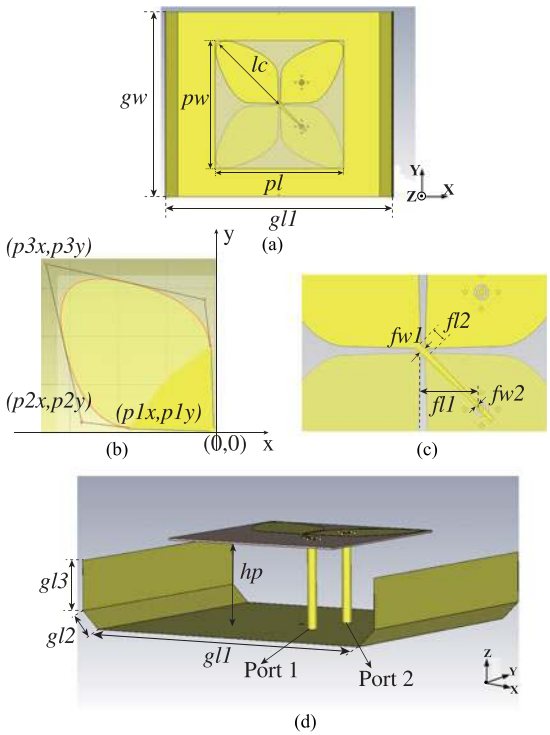

Fig. 1. Configuration of the antenna element. (a) Top view. (b) Definitions of the spline control points for contour of the patch. (c) Local view of the feeding line. (d) Perspective view.

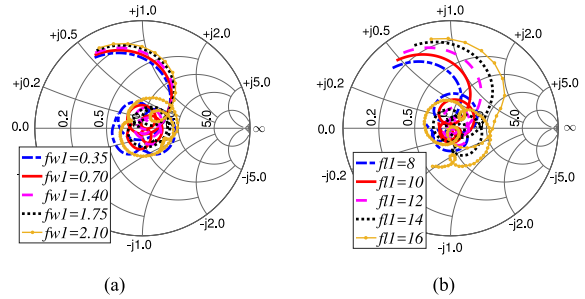

Fig. 2. Simulated reflection coefficients of the antenna element on Smith chart with sweep. (a) *fw1*. (b) *fl1*.

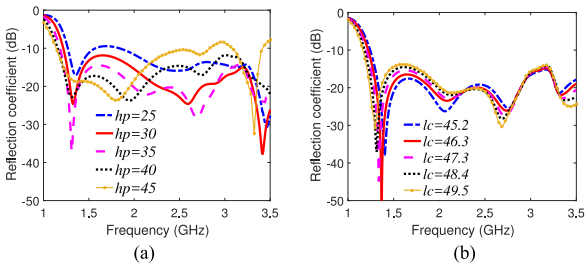

Fig. 3. Simulated reflection coefficients of the antenna element with sweep. (a) *hp*. (b) *lc*.

contoured by a quadratic Bézier spline with four control points. In this way, the limited space is fully used to prolong the current path on the dipole, so that the radiation capability at lower frequency band is improved. Extra degrees of freedom and smooth transition achieved by the spline contour help to realize a good impedance matching over a broad frequency range. To further improve the impedance matching, the feeding line widens gradually from *fw2* to *fw1* as shown in Fig. 1(c), and the tapered feeding line serves as an impedance transformer between the patches and the 50 Ω coaxial cable. To realize dual polarization, two identical bowtie dipoles are perpendicularly placed as depicted in Fig. 1(d), and the -45° and the $+45^\circ$ polarization are excited by port 1 and port 2, respectively. Moreover, both bowtie dipoles and microstrip feeding lines are printed on the substrate of a 0.762 mm thick Arlon AD300 (with dielectric constant of 3.0 and loss tangent of 0.003) to make the antenna fully planar. As shown in Fig. 1(a), one taper of the bowtie dipole is printed on the top side of the substrate, while the other is printed on the bottom side. Finally, as illustrated in Fig. 1(d), the proposed antenna element is placed above a folded reflector to suppress the radiation in sideward directions.

B. Parametric Studies

To well match with impedances of patches, width of the feeding line (*fw1*) should be carefully studied, and the transition length (*fl1*) has a notable effect on the impedance matching as well. It is also noticed through studies that the antenna performance is significantly influenced by the space between the patch and the reflector (*hp*) and the length factor of the tapered patch (*lc*). The four parameters are swept using the CST Microwave Studio, and results are shown in Figs. 2 and 3.

Fig. 2 shows the reflection coefficients of the antenna in a Smith chart, from which it can be seen that *fw1* and *fl1* decide the loop on the track of the reflection coefficient, and the impedance BW can be enhanced by adjusting them. After explorations, it is found that with 50 Ω input impedance, small loops able to be circled by a low reflection coefficient circle is achieved when *fw1*= 1.4 mm and *fl1*= 12 mm.

According to Fig. 3, large *hp* is good for the reflection coefficients at the low band, while the reflection coefficients at high band get worse. Small *hp* leads to opposite results, and thus, *hp* is chosen to be 35 mm as a tradeoff. Besides, small *lc* narrows the band but obtains a lower S_{11} over the operating band, while a large *lc* widens the band with reflect coefficients over the midband lifted up. A large *lc* also increases the antenna size, and therefore, $lc = 49.5$ mm is adopted with the antenna operating band, performance and patch dimensions all taken into consideration.

C. Balanced Structure With Necessary Accessories

When feeding bowtie dipoles with unbalanced coaxial cables, currents on both arms of a dipole are asymmetric, and the leaky current on the outside surface of the coaxial cable will produce undesirable radiation and cause pattern distortion. Fig. 4(a) gives the radiation pattern of the proposed antenna element in the *xz* plane for the two ports. It is noticed that the radiation pattern is not symmetric, and the maximum radiation direction has a derivation from 0°.

It has been demonstrated in [11] that two shorting pins serve as balun and improve the XPD of dual-polarized dipoles fed by coaxial cables. Therefore, in this letter, outer conductors of the feeding cables are mirrored to the antenna center as shown in Fig. 5. The mirrored conductors operate as Pawsey stub baluns to ensure the symmetry of currents on both arms of the bowtie dipole over a very broad BW [12]. Additionally, they also make

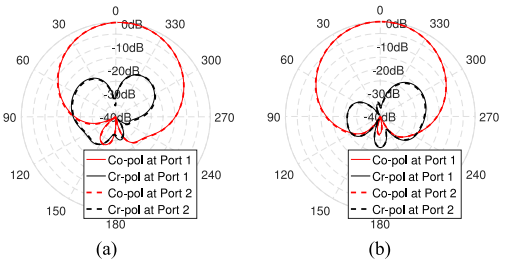

Fig. 4. Simulated radiation patterns of (a) unbalanced and (b) balanced antenna elements in the *xz* plane at 1.9 GHz.

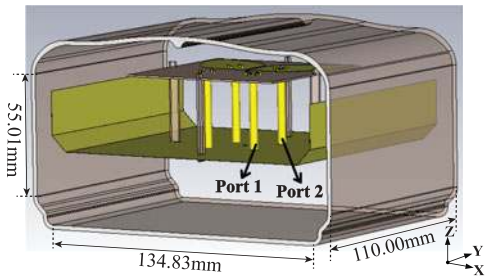

Fig. 5. Geometry of the balanced antenna element with accessories.

TABLE II
OPTIMIZED VALUES FOR THE GEOMETRIC PARAMETERS OF THE BALANCED ANTENNA

Parameter	*gl1*	*gl2*	*gl3*	*gw*	*hp*	*pl*
Value (mm)	120	10	20	110	33	75.4
Parameter	*pw*	*fl1*	*fl2*	*fw1*	*fw2*	*P1x*
Value (mm)	75.4	11	2.8	1.4	0.6	-22
Parameter	*P1y*	*P2x*	*P2y*	*P3x*	*P3y*	*lc*
Value (mm)	1	-28.6	6.5	-46	46	49.5

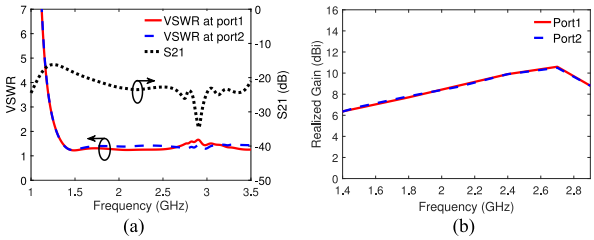

Fig. 6. (a) Simulated VSWRs and port-to-port isolation. (b) Simulated gains of the balanced antenna element with all accessories.

the antenna symmetric in geometry to maintain the mechanical stability.

Furthermore, for practical deployment, four pillars made of 1.2 mm thick FR4 are added to support the patch stably. A radome made of fiberglass and resin (with a permittivity of 4.4 and a loss tangent of 0.02) provided by Huawei Technologies Co., Ltd., is also included to protect the enclosed antenna from the environment. Configurations of the final antenna element with all accessories are illustrated in Fig. 5. The proposed structure is further simulated and optimized, and its final dimensions are summarized in Table II.

Fig. 6(a) shows the VSWR and port-to-port isolation of the whole structure. It can be seen that the VSWR under 1.5 is from 1.35 to 3.5 GHz, except that around 2.7–3 GHz the VSWR at port 1 is under 1.57. The mutual coupling level is under –20 dB across most of the frequency band. According to Fig. 6(b), the gain realized by the antenna element is around 8 dBi.

TABLE III
HPBW, FBR, AND XPD OF THE BALANCED AND UNBALANCED ANTENNA ELEMENTS

Frequency(GHz)		1.427	1.9	2.4	2.9
HPBW (°)	Unbalanced	75	66	53	52
	Balanced	76	69	57	54
FBR (dB)	Unbalanced	21.8	27.2	29.5	23.0
	Balanced	25.9	32.6	34.8	24.6
0° XPD (dB)	Unbalanced	33.5	31.6	26.2	16.2
	Balanced	21.7	36.4	30.8	17.6

Fig. 7. Prototype of the antenna array with 1 × 8 elements.

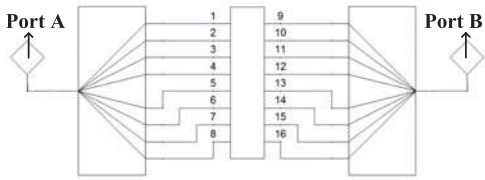

Fig. 8. Network configuration of the antenna array.

Radiation pattern of the balanced antenna element at the two ports is given in Fig. 4(b). From Fig. 4, radiation patterns at port 1 and port 2 are almost identical, wherefore the key evaluation indices, including HPBWs, FBRs, and XPDs, at port 1 at different frequencies for both the preliminary and the balanced antenna elements are summarized in Table III. Compare the results given in Fig. 4 and Table III, it is observed that the main beam direction for the balanced antenna is at 0° and its radiation pattern is more symmetric. In addition, the balanced antenna exhibits more stable radiation pattern, together with improved FBR and XPD, over the entire operating frequency band.

III. EIGHT-ELEMENT DUAL-POLARIZED ANTENNA ARRAY

The proposed antenna element is then extended to an array with 1 × 8 elements. Element spacing in the array is 110 mm ($0.52\lambda_{1.427\,\mathrm{GHz}}$), and the length and width of the reflector are 990 mm × 134.11 mm. A prototype is fabricated as shown in Fig. 7, in which the radome is removed for a clear view.

When measuring the *S*-parameters, all the 16 ports are excited simultaneously with a 24-port vector network analyzer, and a network configuration shown in Fig. 8 is set to investigate the final features of the array. The network contains two 1-to-8 power splitters, each of which connects with the corresponding eight ports exciting the same polarization, and all the −45° polarized ports are excited by port A and the +45° polarized ports are excited by port B.

Fig. 9(a) shows VSWRs of port A and port B and their isolation. Based on the measurement results, from 1.427 to 2.9 GHz, VSWRs at port A and port B are all below 1.5, and isolation between the two ports is lower than −20 dB. The measurement results are consistent with simulation results, and

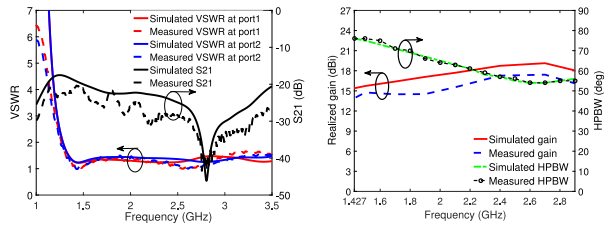

Fig. 9. Measured and simulated. (a) VSWRs and port-to-port isolation. (b) Gain and HPBW in the *xz* plane of the proposed antenna array.

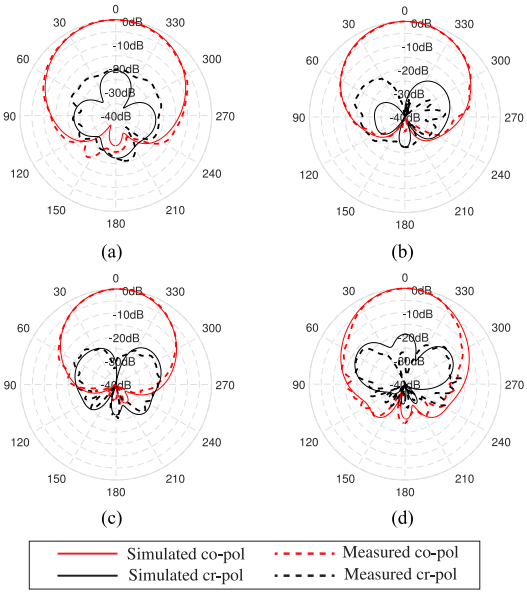

Fig. 10. Simulated and measured radiation patterns of the dual-polarized antenna array in the *xz* plane. (a) 1.427 GHz. (b) 1.9 GHz. (c) 2.4 GHz. (d) 2.9 GHz.

TABLE IV
HPBW, FBR, AND XPD OF THE EIGHT-ELEMENT ANTENNA ARRAY

Frequency(GHz)		1.427	1.9	2.4	2.9
HPBW (°)	Simulation	76	67	57	56
	Measurement	76	66	57	55
FBR (dB)	Simulation	27.4	30.5	31.2	24.9
	Measurement	24.8	33.6	31.4	23.6
0^o XPD (dB)	Simulation	21.2	36.7	31.4	20.1
	Measurement	21.0	40.0	28.3	28.8
Minimum within $\pm 60^o$ XPD (dB)	Simulation	20.4	11.6	8.5	7.1
	Measurement	15.2	9.8	8.0	6.0

minor differences between them come from the fabrication imperfections and effects from the measurement environment.

With a feeding network provided by Huawei Technologies Co., Ltd., radiation pattern at the -45° polarized port in the *xz* plane is measured and plotted in Fig. 10 together with those in simulation for verification. It is observed that the measured results agree well with those in simulation, and discrepancies can be introduced from necessary fixtures and cables of the feeding network. HPBWs of the array are given in Fig. 9(b) and other significant evaluation indicators, including FBR and XPD, are summarized in Table IV. According to the simulation and measurement results, the HPBWs are within 54°–76° over 1.427–2.9 GHz, and the FBRs are higher than 20 dB. Across the entire operating frequency band, XPDs of the proposed antenna array are over 20 dB at the boresight direction, and they are higher than 6 dB from -60° to 60°, which can meet the requirements for base station antennas.

Realized gain of the designed antenna array are plotted in Fig. 9(b). Over 1.427–2.9 GHz, the measured gains are within 13.9–17.4 dBi, which are about 2 dBi lower than the simulated results. Losses can be introduced from the feeding network, SMA connectors, and coaxial cables.

IV. Conclusion

A $\pm 45^\circ$ dual-polarized base station antenna is designed in this letter. Spline-edged bowtie patch and tapered feeding microstrip line are adopted and optimized to achieve broadband impedance matching from 1.427 to 2.9 GHz. Furthermore, Pawsey stub balun structures are added to balance the antenna and improve its radiation properties. An antenna array containing eight elements is then fabricated and measured. The size of the compact base station antenna array is $990 \times 134.11 \times 33.83\,\text{mm}^3$ (excluding a test radome), and over the entire operation band, it realizes HPBW within 54°–76°, XPD and FBR more than 20 dB, and gain from 13.9 to 17.4 dBi. Thanks to its wide operation band and stable radiation performance, the proposed antenna is a strong contender for base stations providing IMT services over various systems.

Acknowledgment

The authors would like to thank Dr. Y. Wu, T. Tang, L. Chen, and D. Daojian for their expert and constructive advice. The authors would also like to thank Dr. M. Munoz Torrico for helping with measurements.

References

[1] International Telecommunication Union, *Provisional Final Acts World Radiocommunication Conference (WRC-15)*, Nov. 2015. [Online]. Available: https://www.itu.int/dms_pub/itu-r/opb/act/R-ACT-WRC.11-2015-PDF-E.pdf

[2] *U.K. Office of Communications*, WRC-07 Agenda Item 1.4, Jun. 2007. [Online]. Available: https://www.ofcom.org.uk/__data/assets/pdf_file/0030/36687/statement.pdf

[3] Y. Gao, R. Ma, Y. Wang, Q. Zhang, and C. Parini, "Stacked patch antenna with dual-polarization and low mutual coupling for massive mimo," *IEEE Trans. Antennas Propag.*, vol. 64, no. 10, pp. 4544–4549, Oct. 2016.

[4] Y. Jin and Z. Du, "Broadband dual-polarized f-probe fed stacked patch antenna for base stations," *IEEE Antennas Wireless Propag. Lett.*, vol. 14, pp. 1121–1124, 2015.

[5] Y. Luo and Q. X. Chu, "Oriental crown-shaped differentially fed dual-polarized multidipole antenna," *IEEE Trans. Antennas Propag.*, vol. 63, no. 11, pp. 4678–4685, Nov. 2015.

[6] Y. Liu, H. Yi, F. W. Wang, and S. X. Gong, "A novel miniaturized broadband dual-polarized dipole antenna for base station," *IEEE Antennas Wireless Propag. Lett.*, vol. 12, pp. 1335–1338, 2013.

[7] Y. Cui, R. Li, and H. Fu, "A broadband dual-polarized planar antenna for 2G/3G/LTE base stations," *IEEE Trans. Antennas Propag.*, vol. 62, no. 9, pp. 4836–4840, Sep. 2014.

[8] Z. Bao, Z. Nie, and X. Zong, "A novel broadband dual-polarization antenna utilizing strong mutual coupling," *IEEE Trans. Antennas Propag.*, vol. 62, no. 1, pp. 450–454, Jan. 2014.

[9] Y. Cui, R. Li, and P. Wang, "A novel broadband planar antenna for 2G/3G/LTE base stations," *IEEE Trans. Antennas Propag.*, vol. 61, no. 5, pp. 2767–2774, May 2013.

[10] L. J. Chu, "Physical limitations of omni-directional antennas," *J. Appl. Phys.*, vol. 19, no. 12, pp. 1163–1175, 1948.

[11] Y. Luo, Q. X. Chu, and D. L. Wen, "A plus/minus 45 degree dual-polarized base-station antenna with enhanced cross-polarization discrimination via addition of four parasitic elements placed in a square contour," *IEEE Trans. Antennas Propag.*, vol. 64, no. 4, pp. 1514–1519, Apr. 2016.

[12] C. A. Balanis, "Microstrip antennas," in *Antenna theory: Analysis and Design*, 3rd ed. Hoboken, NJ, USA: Wiley, 2005.